

NIS
11-23-77
377475
p.17

A Proposed X-Ray Interferometer
for
Measurement of Phases
of
Diffracted X-Rays

Hong-Yee Chiu
Institute for Space Studies
Goddard Space Flight Center, NASA
New York, New York 10025

and

Celia C. Chiu
St. Lukes Hospital Center
New York, New York 10025

(NASA-TM-103018) A PROPOSED X RAY
INTERFEROMETER FOR MEASUREMENT OF PHASES OF
DIFFRACTED X RAYS (NASA) 17 P

N90-71337

Unclas
00/35 0277475

Presented at Intercongress Symposium "Direct Methods in
Crystallography", sponsored by the International Union of
Crystallography and the Medical Foundation of Buffalo, New
York, August 3-6, 1976.

I. Introduction and Interferometer Principle.

Since what will be presented below is drastically different from the rest in this symposium, a few words might be appropriate to justify the presence of this paper. As the title suggested, we are proposing to build an X-ray interferometer to accurately measure the variation in intensity caused by the phase difference between interfering X-ray beams, and to deduce the phase difference from these measurements. From our preliminary feasibility studies based on published results, we realize the determination of phase relationships through intensity measurements will be a very time consuming affair. With the undeniably fantastic success of the statistical method, we feel the most efficient way to do structural analysis for large molecules may be to measure the phases for a handful of crucial reflections and leave the rest to the statistical method.

X-ray interferometer is not a white elephant. In the 1960's a whole series of X-ray interferometers were built by Bonse and Hart¹ then at Cornell University, using the Borrmann effect as a beam splitting mechanism. As shown in Figure 1, a beam of X-rays incident upon a thick perfect crystal at the Bragg angle to a set of lattice planes, a standing wave pattern is set up inside the crystal and a pair of coherent beams emerged at the other surface of the crystal (Borrmann effect). The angle between the pair of coherent beams is twice the Bragg angle. Bonse and Hart were successful in recombining these two beams to produce interference patterns. However, in all their designs, the angle of recombination is always the same as the beam splitting angle. The design we propose offers a continuously variable angle of recombination. In order to fulfill

interference conditions, the following conditions must be met:

(1) A pair of beams originating from the same source point must intersect at some later point in space.

(2) The phase difference between all pairs of beams must be the same.

(3) The absolute path differences between the pairs must not exceed the correlation length of the photon.

Figure 2 shows our design.² A single perfect crystal is carved into an L shaped slab with two perpendicular sides R and T. R is parallel and T is perpendicular to a set of selected lattice planes LP. An incident ray is evenly split into two beams I_1 and I_2 by T. One of the these two beams, I_1 , is directed towards R. Upon Bragg reflection from the set of lattice planes of R,³ I_1 becomes I_1' which is almost parallel to I_2 . I_1' and I_2 are related by a mirror symmetry.

If a plane normal to I_1' and I_2 is introduced, the path length of both I_1' and I_2 to this plane is source point dependent. In order to eliminate the source position dependence, a pair of wedges are introduced which causes I_2 to traverse an extra path through bending and rebending. The geometry of the wedges is such that the difference in the path lengths of I_1' and I_2' , the transmitted I_2 , becomes source position independent. By adding multiple reflection path extenders and adjustments of the position of the wedges, the path lengths I_1 and I_2 can be made to be identical (at least theoretically). Because of the presence of the wedges, the intensities of I_1' and I_2' will differ and that of I_2' will be source dependent. Appropriately shaped absorbers can be used to correct these differences.

I_1' and I_2' then fall onto two sets of lattice planes (mirrors) M_1 and M_2 , which are mounted in such a way that they always satisfy Bragg reflection conditions and can rotate about an axis in central directions of I_1' and I_2' . By suitable adjustments it is possible to bring the two reflected rays R_1 and R_2 to intersect at T , with a continuously variable angle of intersection δ . Because of the symmetry in design, all pairs of rays intersect with the same path difference, and all the intersecting points lie on the bisecting plane of I_1' and I_2' .

After Borrmann transmissions and subsequent reflections and transmissions, the bandwidth of I_1 and I_2 are sufficiently small, and their directions are well defined to within a few seconds of arc. Theoretically calculated photon correlation length is of the order of 30μ for a beam width of one second of arc. Bonse and Hart reported that coherence is achieved at 10μ and disappears at 100μ .⁴

II. Geometry of Diffraction.

The geometry of diffraction is shown in Figure 3. The sample crystal is located at the intersection point of I_1 and I_2 . The angle of intersection δ is chosen that upon entering the sphere of reflection both ends of a selected reciprocal vector H_0 serve as origins of reciprocal lattices for the two rays I_1 and I_2 . The crystal is rotated about an axis h_0 which is parallel to H_0 , and both h_0 and H_0 are perpendicular to the bisecting plane of I_1 and I_2 . The origin of the crystal lattice is then defined as the intersection of h_0 and the bisecting plane of I_1 and I_2 . As the crystal rotates about h_0 , at a certain angle, a reciprocal lattice point P will pass through

the surface of the sphere of reflection defined by \underline{H}_0 , I_1 , and I_2 . Both I_1 and I_2 will be diffracted in the direction of TP, by two corresponding sets of planes \underline{H}_1 and \underline{H}_2 such that $\underline{H}_1 - \underline{H}_2 = \underline{H}_0$. If an appropriate \underline{H}_0 is chosen, a whole collection of simultaneous reflections among pairs of planes \underline{H}_A and \underline{H}_B such that $\underline{H}_A - \underline{H}_B = \underline{H}_0$ can be determined from a single setting of δ .

We can measure the intensity of reflection \underline{H}_1 by blocking I_1 , and the intensity of $\underline{H}_2 = \underline{H}_1 + \underline{H}_0$, by blocking I_2 . Then we can measure the intensity along TP when the two rays are simultaneously incident upon the crystal. In general, the intensity of the combined beams \underline{H}_1 will not be equal to the sum of the independent beam intensities. It is possible to deduce the phase difference ψ of the two reflected beams from the intensity measurements via the following equation:

$$\cos \psi = \frac{|\underline{E}_{H12}|^2 - |\underline{E}_{H1}|^2 - |\underline{E}_{H2}|^2}{2|\underline{E}_{H1}| \cdot |\underline{E}_{H2}| \cdot \cos \gamma_c} \quad (1)$$

where γ_c is the angle between polarization of the two simultaneously reflected beams, and the E's are the amplitudes of reflections after suitable crystallographic corrections (e.g. Lp factors).

III. Feasibility.

The question naturally arises as to the technical feasibility for the construction of the proposed instrument. Bonse and Hart showed that it is possible to construct an interferometer out of separate perfect crystal blocks. In our case the problem is complicated by the fact that the beam path corrector has to correct beam paths to a fraction of λ : The accuracy of the determined value of the phase is 2π times the ratio of uncertainties in the position of the relative wave fronts to the wavelength. If a typical value of λ is 1.5 \AA , in order to determine the phases to within 36° it is

necessary to maintain the wave front difference to within a linear dimension of 0.15 \AA . The following problems are encountered in this consideration: (1) Means of monitoring sub- \AA dimensional changes as well as making corresponding corrections. (2) Temperature and vibration effects. In addition, one must consider (3) The adequacy of the intensity of the two interfering beams for a meaningful set of data within a reasonable amount of time.

Techniques for measurement of sub- \AA dimensional changes have been developed for precision optics in large telescopes. Using tunable lasers, optical cavities can be used to measure linear dimensional to an accuracy of one part in 10^{11} or better.⁵ Figure 4 shows a conceptual design for the measurement and monitoring dimensional changes of crucial parts of the interferometer. The solid lines indicate X-ray paths and the dotted lines indicate laser paths. Fortunately, the correction of X-ray paths to sub- \AA accuracies is greatly facilitated by the fact that the refractive index for X-rays in all materials is very close to unity. Therefore, should there be a change in the path lengths, we can correct the changes by inserting suitable phase retardation plates of reasonable thickness. (For a deviation from unity of the refractive index by 10^{-6} , a phase lag of 2π is introduced by a retardation plate of around 150μ in thickness for the Cu K α radiation.

Materials have been developed for low thermal expansion coefficients. Figure 5 shows the thermal expansion coefficient for various low expansion materials.⁶ It is interesting to note that a number of these materials achieve zero expansion at some reasonable temperature.

Further, two of these materials, ULE (a nonmetal) and superinvar (a metal) have the same zero expansion temperature (around 45°C).

Relief of internal strains in the course of time will cause temperal changes in dimensions. Studies of long term dimensional stability of materials have been carried out by Jacobs et al.⁷ Figrues 6 and 7 shows the dimensional stability of ULE and superinvar. It appears that two to six months are necessary for these materials to reach dimensional stability. However, this may not be a true dimensional change but merely reflecting the shortcomings of the measuring methods.

Vibration effects can be eliminated by sitting the instrument on an air bag in a sand pit. This is a well established technology.

The single most difficult problem remains the adequacy of intensity. Based on published results using conventional X-ray generators, our estimate for the the weaker beam (I_2') is about 150 counts/second, and the diffracted beam from I_2' is then about 130 counts / day assuming a diffraction factor of 10^{-5} .² However, if synchrotron radiation does live up to the claim of increasing available beam intensity by a factor of 10^4 , the counting rate of the diffracted beam will be increased to 10^3 counts/min. It should be pointed out that only in recent years has synchrotron radiation been considered seriously for X-ray diffraction studies. The art of producing intense X-ray beams for diffraction studies from a synchrotron is still at its infancy.

4. Conclusion.

In this paper we have departed from conventional approach and proposed an interferometer as an alternate solution to the phase problem. Granted that technological problems are severe, but the

solution to these technological difficulties are already in existence. Further, even if X-ray lasers can be successfully developed in the future, the interferometer described in this paper (or a similar type) is the necessary first step towards the solution of the phase problem.

References.

1. Bonse, U. and Hart, M. Applied Phys. Lett., 6, 155 (1965)
Z./ Physik, 188, 154 (1965), 190, 455 (1966), 194, 1, 455(1966).
2. "Interference in Mosaic Crystals and the Empirical Determination of Phases of Diffracted X-rays", C. C. Chiu and H. Y. Chiu, (Submitted to the Physical Review, 1976).
3. It is necessary to flex the reflection surface by a small amount to accomodate a small change in the Bragg angle due to refraction.
4. Bonse, U. and Hart, M., Z. Physik, 214 (1968).
5. Some of these techniques are described in an article by Jacobs, S. F., Bradford, J. N., and Berthold III, J. W., Applied Optics 9, 2477 (1970).
6. See references quoted in 5.
7. "Measurement of Dimensional Stability", Jacobs, S. F., Berthold III, J. W., Norton, M.. Final report under NASA contract NAS 8-28661.

Figure Captions

- Figure 1. Borrmann effect. An incident beam at Bragg angle θ_0 with the set of planes LP sets up wave fields and propagate along LP in the beam splitter crystal BS. At the exit surface the wave field is split into two beams TR and FD which propagate to two opposite directions, with an angular separation of $2\theta_0$. The direct transmitted beam DT is suppressed by normal absorption.
- Figure 2. Schematic diagram of an interfero-diffractometer.
- Figure 3. Geometry of simultaneous diffractions of two coherent beams into a common direction.
- Figure 4. A conceptual design for monitoring dimensional changes in the interferometer. Solid lines represent X-ray paths and dotted lines represent laser paths. A rotating wheel CW is used to make path corrections through retardation of phases.
- Figure 5. Thermal expansion coefficients of a number of low expansion materials. Note that several materials pass through zero thermal expansion phase.
- Figure 6. Dimensional stability of ULE. The ordinate is the tuning frequency that is necessary to satisfy the optical cavity conditions. Generally the accuracy of measurement is around $d\Delta\nu/\nu_0$ where ν_0 is the laser frequency and is in the range of 10^{16} .
- Figure 7. Dimensional stability of superinvar. See captions in Figure 6 for explanations.

Chiu + Chiu 030652 PR

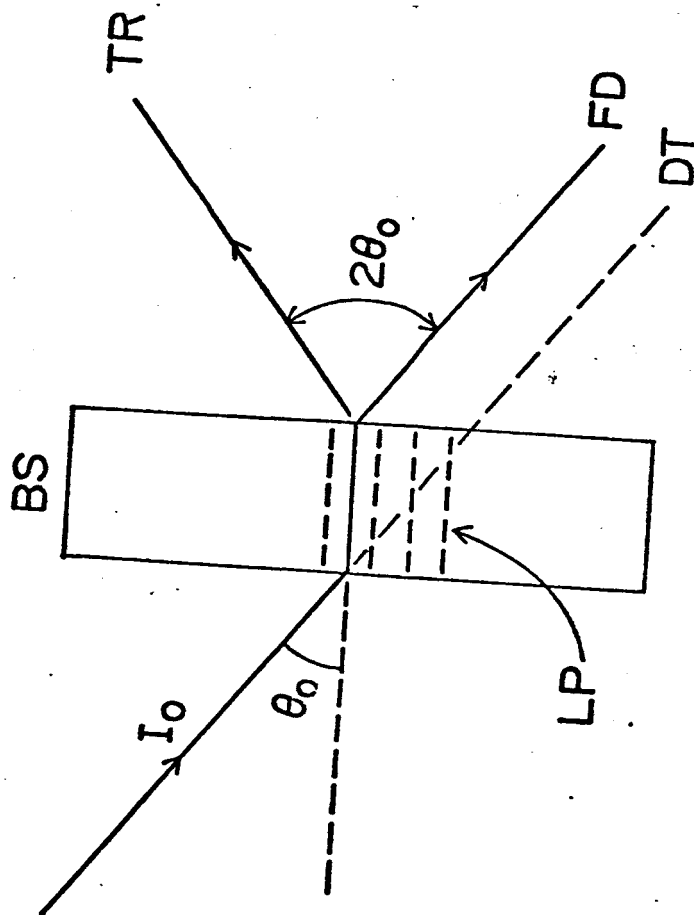


Figure 1 - Borrmann effect

Figure 1

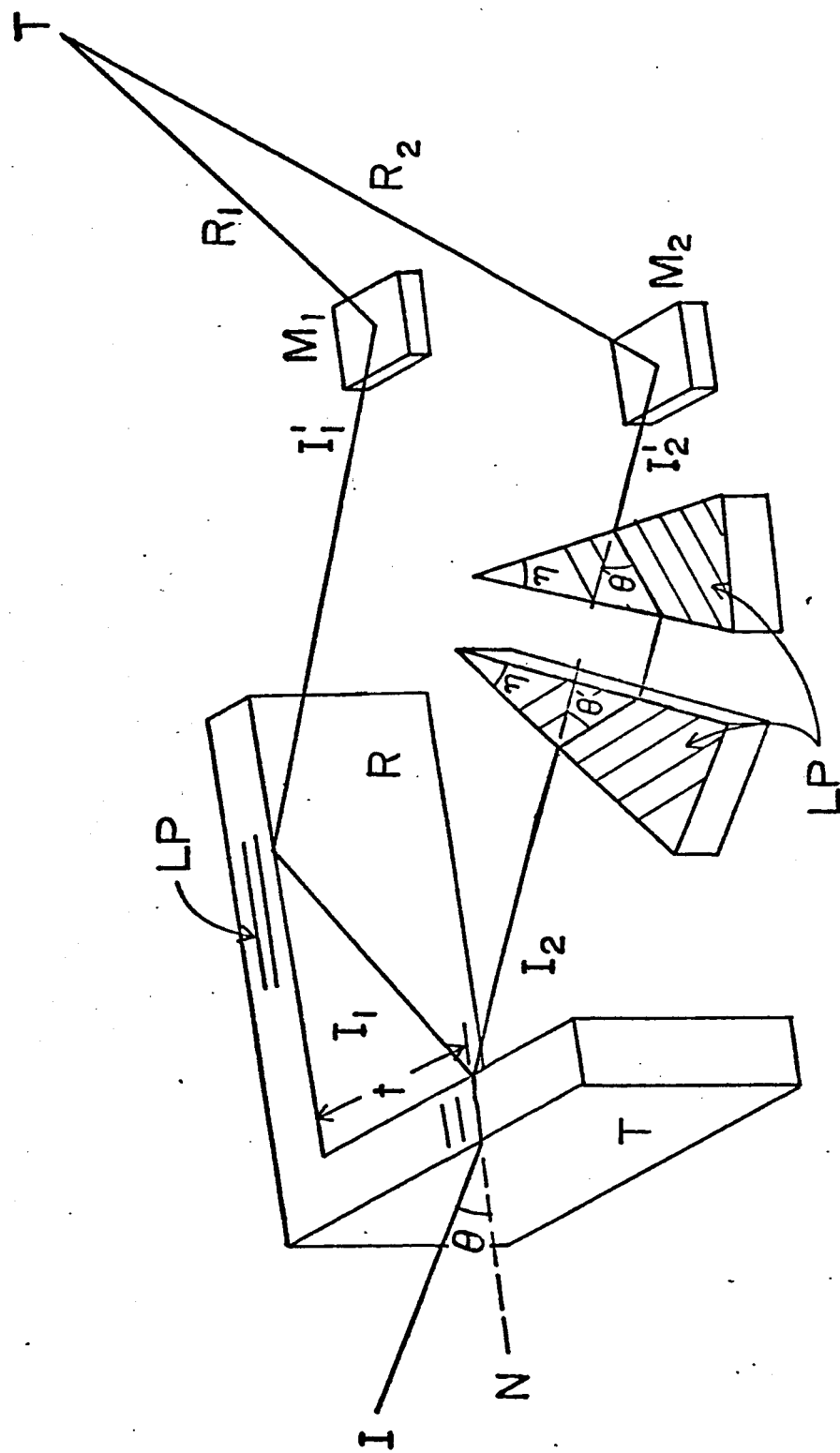


Figure 2- Interfero-diffractometer Configuration

Chen + Chen 00000000

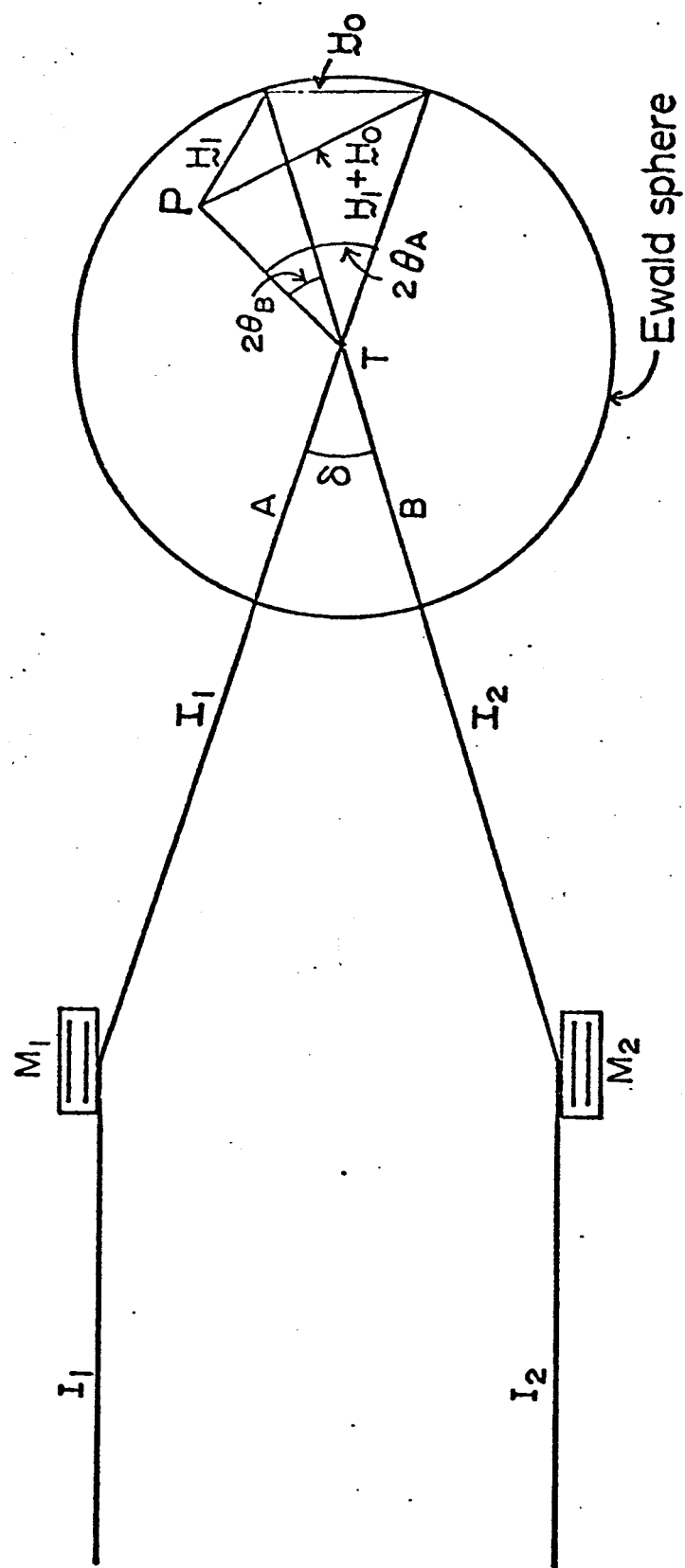


Figure 3

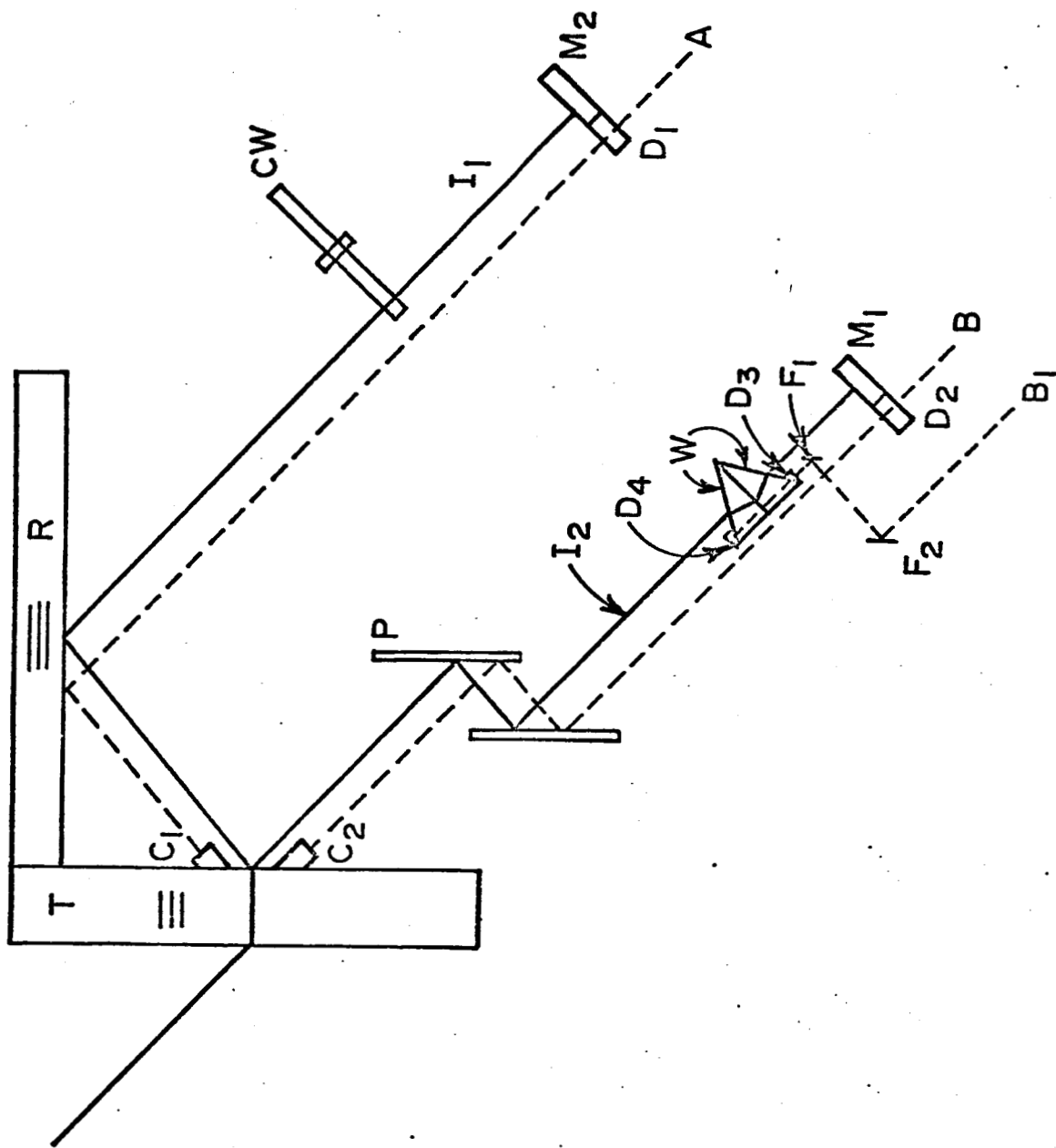


FIG 4

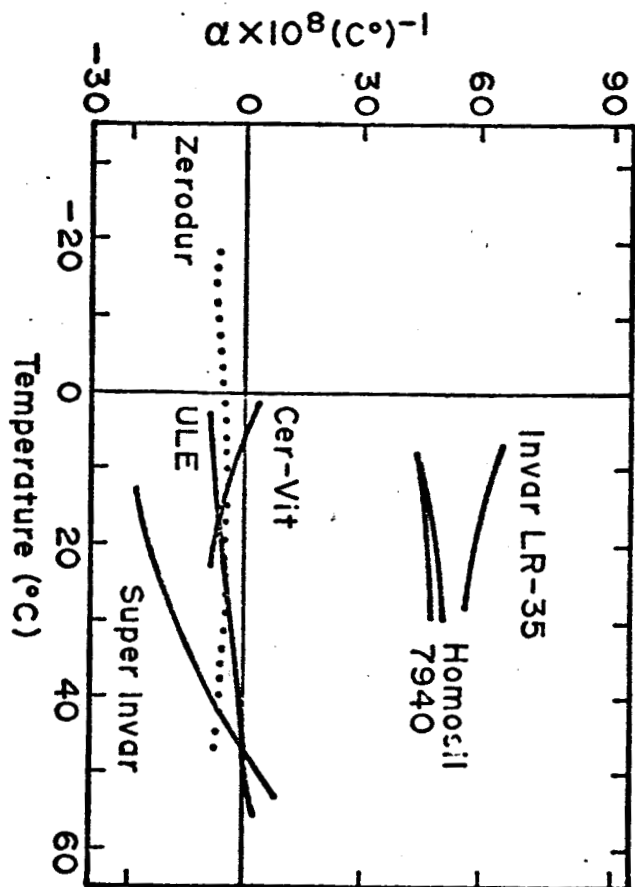


Figure 5

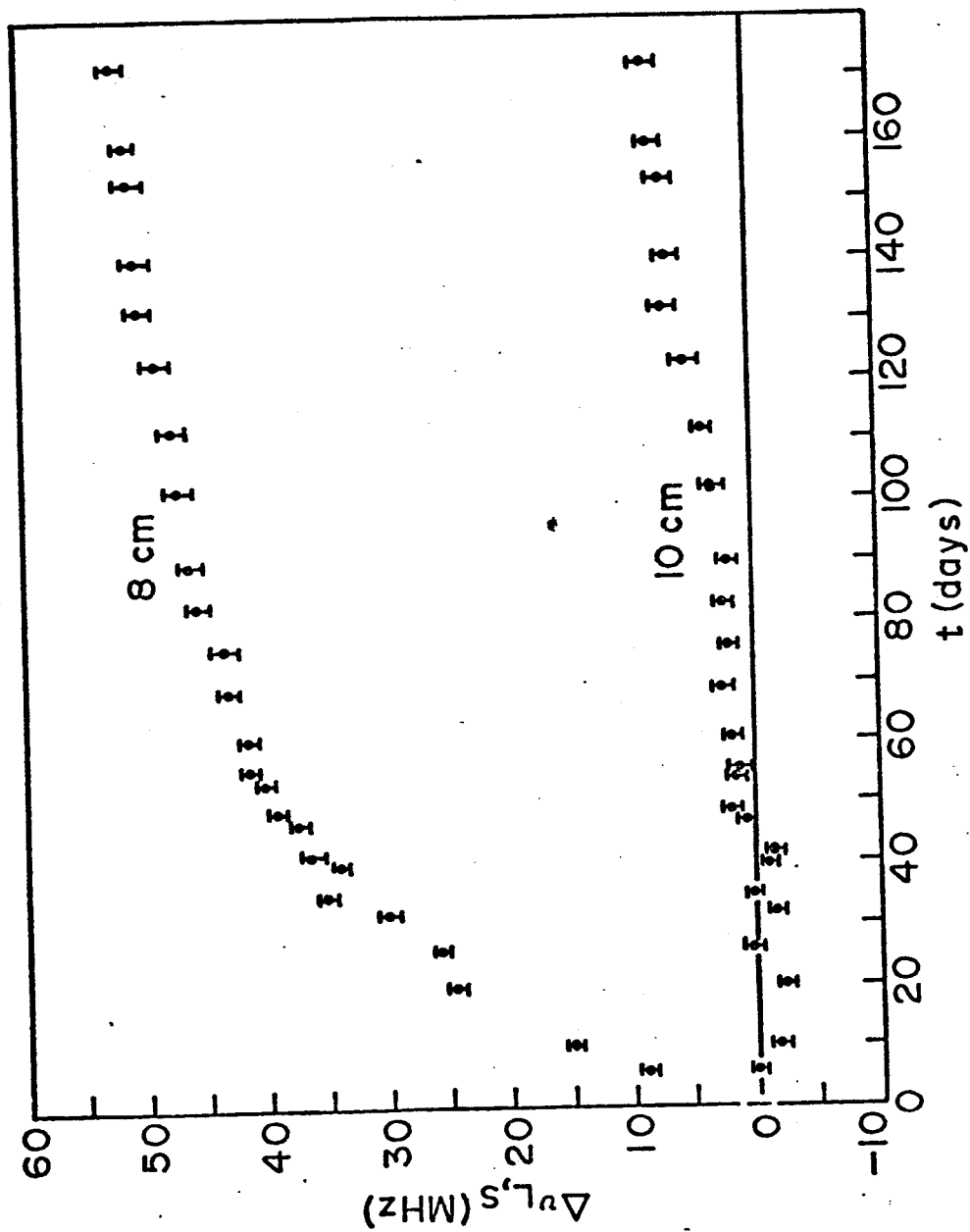


Figure 1

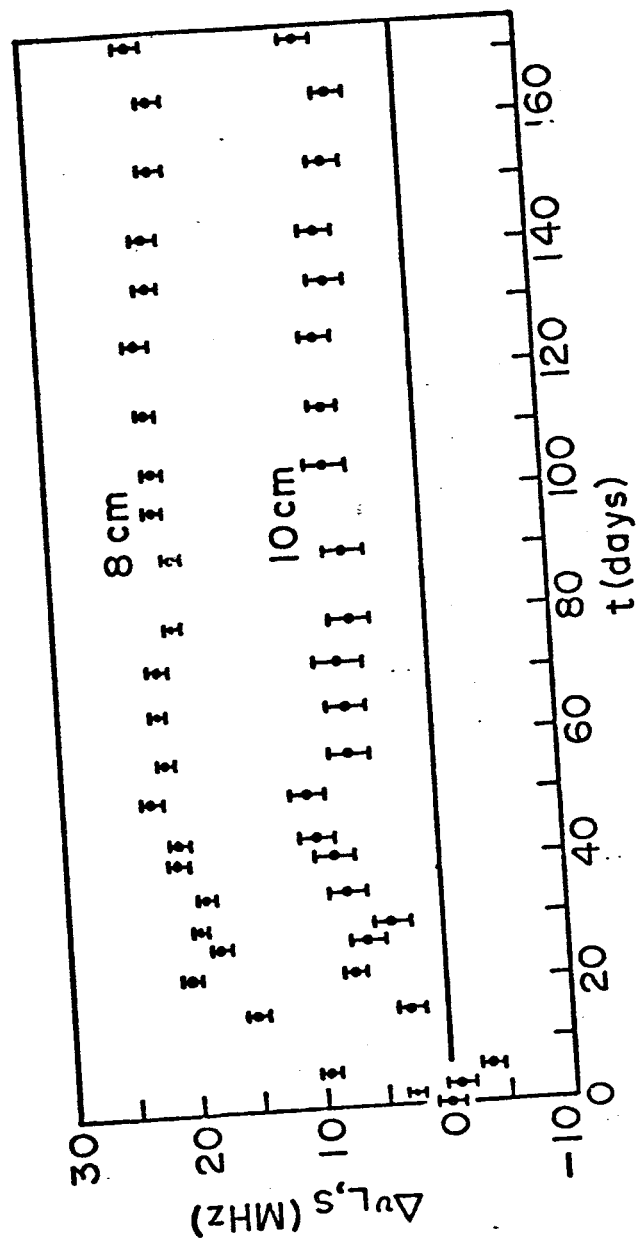


Fig 7